


Original article



## Chronic motoneuronal activation enhanced axonal regeneration and functional recovery after brachial plexus injury

Shiqin Lv<sup>a</sup> , Zizhuo Wu<sup>a</sup>, Yu Huang<sup>a</sup>, Pingzhen Wu<sup>a</sup>, Jianqing Shao<sup>a</sup>, Jiajia Wu<sup>a</sup>, Ke Zhong<sup>d</sup>, Lihua Zhou<sup>a,\*</sup>, Wutian Wu<sup>b,c,\*\*</sup>

<sup>a</sup> Department of Anatomy, School of Medicine (Shenzhen), Sun Yat-sen University, Shenzhen, Guangdong, 518107, China, No.66, Gongchang Road, Guangming District, Shenzhen, Guangdong, 518107, China

<sup>b</sup> Guangdong-Hong Kong-Macau Institute of CNS Regeneration, Ministry of Education Joint International Research Laboratory of Central Nervous System Regeneration, Jinan University, Guangzhou, Guangdong, 510632, China, No.601, West Huangpu Avenue, Tianhe District, Guangzhou, Guangdong, 510632, China

<sup>c</sup> Jiangsu RE-STEM Biotechnology Co., Ltd., Building A1, Yuewang Zhihui, 1463 Wuzhong Avenue, Suzhou, Jiangsu, 215104, China

<sup>d</sup> Department of Pharmacy, Sun Yat-Sen Memorial Hospital, Sun Yat-Sen University, Guangdong, 510102, China, No. 107, Yanjiang West Road, Yuexiu District, Guangzhou, Guangdong, 510102, China

### ARTICLE INFO

#### Keywords:

Chemogenetic activation  
Spinal motoneurons  
Brachial plexus injury  
Motor repair

### ABSTRACT

**Background:** Brachial plexus injury (BPI) leads to significant impairment of upper limb motor function, primarily due to progressive atrophy of denervated muscles resulting from the slow rate of axonal regeneration. Therefore, identifying strategies to accelerate axon extension is of critical importance.

**Methods:** In this study, we first established a mouse model of brachial plexus injury and employed chemogenetic approaches to specifically activate C6 spinal motoneurons. We then assessed axonal regeneration and motor function recovery in the injured mice through behavioral tests, morphological analyses, and electrophysiological detection.

**Results:** We found that the AAV9-hM3Dq virus efficiently transduced motoneurons, and CNO administration robustly activated mature hM3Dq<sup>+</sup> motoneurons in vivo. Chronic chemogenetic activation significantly enhanced the regeneration of spinal motoneurons injured by ventral root crush, accelerated axon extension, and improved axonal myelination, resulting in increased axon size. This activation also facilitated the formation of new neuromuscular junctions (NMJs) in adult motoneurons and reduced muscle atrophy. Furthermore, it promoted electrophysiological recovery of the motor unit and improved overall motor function.

**Conclusion:** Chemogenetic activation of adult motoneurons can robustly enhance axon growth and mediate better behavioral recovery. These findings highlight the therapeutic potential of chemogenetic neuronal activation in promoting functional recovery following nerve injury.

**The translational potential of this article:** We have established a chronic chemogenetic method to activate hM3Dq<sup>+</sup> motor neurons after brachial plexus injury, which accelerates axonal regeneration and enhances functional recovery. This strategy holds promise as a clinical therapeutic approach for treating nervous system injuries.

### 1. Introduction

Adult traumatic brachial plexus injury is regarded as one of the most devastating lesions of peripheral nerve injury, characterized by

pathological changes such as axonal degeneration, axoplasmic transport arrest, Schwann cell damage, nerve fiber demyelination and complete Wallerian degeneration [1,2]. Although surgery as an important treatment has significantly changed the outcome of BPI with advances in

\* Corresponding author.

\*\* Corresponding author. Guangdong-Hong Kong-Macau Institute of CNS Regeneration, Ministry of Education Joint International Research Laboratory of Central Nervous System Regeneration, Jinan University, Guangzhou, Guangdong, 510632, China, No.601, West Huangpu Avenue, Tianhe District, Guangzhou, Guangdong, 510632, China.

E-mail addresses: [lvshq5@mail2.sysu.edu.cn](mailto:lvshq5@mail2.sysu.edu.cn) (S. Lv), [wuzizhuosysu@sina.com](mailto:wuzizhuosysu@sina.com) (Z. Wu), [huangy695@mail2.sysu.edu.cn](mailto:huangy695@mail2.sysu.edu.cn) (Y. Huang), [wupzh9@mail2.sysu.edu.cn](mailto:wupzh9@mail2.sysu.edu.cn) (P. Wu), [shaojq@mail2.sysu.edu.cn](mailto:shaojq@mail2.sysu.edu.cn) (J. Shao), [wujj226@mail2.sysu.edu.cn](mailto:wujj226@mail2.sysu.edu.cn) (J. Wu), [zhongk9@mail.sysu.edu.cn](mailto:zhongk9@mail.sysu.edu.cn) (K. Zhong), [zhoulih@mail.sysu.edu.cn](mailto:zhoulih@mail.sysu.edu.cn) (L. Zhou), [wtwu@hku.hk](mailto:wtwu@hku.hk) (W. Wu).

<https://doi.org/10.1016/j.jot.2025.02.007>

Received 28 November 2024; Received in revised form 23 February 2025; Accepted 27 February 2025

2214-031X/© 2025 The Authors. Published by Elsevier B.V. on behalf of Chinese Speaking Orthopaedic Society. This is an open access article under the CC BY-NC-ND license (<http://creativecommons.org/licenses/by-nc-nd/4.0/>).

micro-neurosurgery over the past few decades, the clinical prognosis is suboptimal due to the limited ability of axons to regenerate over long distances and the following irreversible muscle atrophy [3]. Therefore, interventions other than procedure are quite important.

As we all know, intrinsic growth capacity of injured motoneurons is a determinant of axon regeneration, which dictates a battery of injury responses in axons and cell bodies [4,5]. Unfortunately, lesions of proximal spinal nerves like BPI fail to arouse a robust regenerative response due to great loss of motoneurons and limited regenerative ability of remaining neurons. Numerous studies have demonstrated various approaches to enhance intrinsic growth ability of neurons, including pharmacological treatment and neurotrophic factor delivery [6,7]. In our previous study, we found that small peptides like intracellular sigma peptide (ISP) and phosphatase and tensin homolog agonist protein (PAPs) can remarkably promote axon regeneration and function restoration after BPI [8]. Notably, another potential approach that has been explored to enhance the intrinsic ability for long distance nerve fibers regrowth is neuronal activation. Epidural electrical stimulation can promote axon regeneration and functional recovery after peripheral nerve injury [9–11]. However, electrical stimulation faces significant technical limitations such as relatively poor neuronal types targeting and the inconvenient cable connections when used on patients [12,13]. Therefore, developing other methods that can achieve the same goal is challenging but promising [14].

Some research have been demonstrated that remote activation of neurons expressing excitatory design receptors activated by the engineered drug (DREADD) hM3Dq by using the receptor's ligand chlorpyrimidine-N-oxide [15] (CNO) can greatly improve retinal ganglion cell axonal outgrowth after optic nerve crush injury [16,17]. Moreover, DREADD-induced specific and continuous stimulation of transplanted human induced pluripotent stem cell derived neural stem/progenitor cells (hiPSC-NS/PCs) [18] and dorsal root ganglion (DRG) neurons [19] can respectively facilitate new synapse formation following spinal cord injury and enhance axon grow across the dorsal root entry zone after dorsal root crush injury. However, it remains unknown whether enhancing the activity of motoneurons after BPI can promote axon regeneration and functional restoration.

Activation of neurons using chemogenetics techniques is a convenient and specific approach, as the hM3Dq gene can be specifically expressed in any neuron with the help of viral tools, and subsequent chronic activation of neurons over a long period of time is simply administrated by CNO, which can penetrate the blood–brain barrier [15]. Here, we hypothesized that long-term consecutive activation of mature motoneurons by hM3Dq expression might be a potential therapeutic approach for brachial plexus injury. To confirm this hypothesis, we first optimized the BPI surgical model from ventral root avulsion to a more stable crush surgery model. This model rendered the C6 ventral nerve as the sole conduit linking the spinal cord to the biceps for subsequent observations, as our previous study had demonstrated [8]. We demonstrate that chronic motoneurons activation can remarkably promote motor function restoration of the completely-transected spinal nerves, as evidenced by morphological observation of the musculocutaneous nerve and biceps, electrophysiological verification and also the behavioral tests of injured animal. Our results provide the potential effective strategy for treating severe peripheral nerve injuries, promoting nerve regeneration and motor function recovery.

## 2. Materials and methods

### 2.1. Animals and virus preparation

Young Adult female C57BL/6 mice (20–23 g) provided by the Laboratory Animal Center of Sun Yat-sen University were used for the present study. All mice were housed under standard temperature-controlled conditions with a 12/12-h light–dark cycle with ad libitum access to water and food. The animal care and experimental procedures

of this study were approved by the Laboratory Animal Ethics Committee of Sun Yat-sen University (Approval number: SYXK 2017-0081) and are in accordance with guidelines for the ethical review of laboratory animal welfare (GB/T 35892-2018). Injured animals were randomly assigned to cages for follow-up double-blind trials.

The AAV9 virus is produced by Vigene Bioscience (Jinan, China). We chose the adeno-associated virus serotype 9 vector (pAV-CMV-P2A-GFP) to express the mouse hM3Dq gene, which is controlled by the CMV promoter. On the other hand, we used an AAV9 vector expressing GFP as a control virus.

### 2.2. Intraspinal injection of AAV9 virus

Mice were under deep anesthetic state by continuous supplying 1 % isoflurane (RWD, Shenzhen, China) and fixed on a stereotaxic apparatus. We carefully exposed the C6 spinal cord segment followed by removal of cervical vertebra and dura under deep anesthetic state by continuous supplying 1 % isoflurane, and then fixed the mouse on a stereotaxic apparatus. AAV9-hM3Dq-GFP or AAV9-GFP virus was diluted to the same final titer of  $6 \times 10^{12}$  vg/mL and stereotaxically injected into the right ventral horn using a fine glass micropipette attached to Nanoject III (Drummond Scientific, Broomall, USA). With the aid of a stereotaxic apparatus, adjust the needle insertion site, i.e., 0.5 mm lateral to the midline and 1.0 mm deep to the spinal cord surface, and then carefully insert the glass micropipette into the exposed spinal cord. A total of two sites 1 mm apart were injected into the C6 right ventral horn. For each site, 500 nL of virus diluents were administrated at the speed of 3 nL/s, and the micropipette should be held in ventral horn for another 3 min to avoid virus reflux.

### 2.3. Characterization of AAV9 expression

A weeks after AAV9-hM3Dq-GFP or AAV9-GFP virus injection, we harvested C6 spinal cord and then cut it into cross-section at a thickness of 20  $\mu$ m with a Cryostat (Thermo NX50; Thermo Fisher Scientific, Massachusetts, USA) and mount on Superfrost Plus slides (CITOTEST, Jiangsu, China). Before antibody incubation, the sections were sequentially washed with PBS (three times, 5min for each) and 0.3 % PBS-Triton-100 (three times, 15min for each). Immediately, sections were incubated with goat ChAT antibodies (1:500, Millipore, Burlington, MA, USA). After overnight incubation at 4 °C, sections were then immunostained with secondary antibodies Alexa Fluor 546-conjugated donkey anti-goat IgG (1:1000; Thermo Fisher Scientific, Waltham, MA, USA) for 2 h in room temperature. Images were obtained with fluorescence microscope (Leica DM6B, Leica, Wetzlar, Germany).

### 2.4. Quantification of ventral horn c-Fos expression induced by CNO administration

A week after intraspinal injection of AAV9-hM3Dq-GFP or AAV9-GFP, animals were intraperitoneally injected with 1 mg/kg CNO (APEXIO Technology LLC, Houston, USA; 1 mg/mL in 0.5 % DMSO/0.9 % saline) and perfused 2 h later. To visualize c-Fos expression, spinal cord sections were incubated with rabbit monoclonal c-Fos antibody (1:500, cat#2250, Cell Signaling Technology, Massachusetts, USA), an established methods to confirm chemogenetic neuronal activation, overnight at 4 °C followed by incubation with AlexaFluor 546-conjugated donkey anti-Rabbit secondary antibody (1:1000; Cat# A10040, Thermo Fisher Scientific, USA) for 2 h at room temperature. GFP<sup>+</sup> neurons that also express c-Fos<sup>+</sup> was counted and compared between two groups. 6 slides of each animal were analyzed.

### 2.5. Brachial plexus root crush injury

After AAV9 injection, mice were subjected to C6 spinal ventral root crush injury, which was following the same surgical procedure of

previously description [8]. First, the mouse is anesthetized using 1 % isoflurane (RWD, Shenzhen, China), and then the cervical spinal cord will be exposed by using No. 15 scalpel. After that, to better expose the right C5-7 spinal nerve, we removed the right lamina of the cervical segment using a fine rongeur and opened the dura by using ophthalmic scissors. Without damaging the spinal cord, we avulsed the C5 and C7 ventral root with a homemade fine glass hook, and then completely trim away C5 and C7 spinal nerve to prevent extra regeneration. Taking care to avoid epineurial rupture, crush the remaining C6 ventral root three times at the same site and with the same force (10 s each time). The crush site should be as close to the root as possible without injuring the spinal cord. After the procedure, muscle and skin were sutured in layer. Mice were gently placed on a thermostatic heating pad until they fully recover from anesthesia. For that record, our model guarantees that the C6 ventral root is the only connection between spinal cord and the biceps.

## 2.6. Grouping and CNO administration

Mice of sham group were received AAV-GFP injection and sham surgery, while mice in hM3Dq and GFP groups were received AAV9-hM3Dq-GFP or AAV9-GFP injections, respectively, and then these two groups of mice were subjected to the same C6 spinal ventral root crush surgery. All animals were subjected to intraperitoneal injection of CNO (1 mg/kg each time for each mouse) every evening starting the day a week post viral injection to the day before sacrifice. In addition, all behavioral experiments should be performed prior to that day's CNO administration to exclude post-dose effects.

## 2.7. Behavioral testing

### 2.7.1. Terzis grooming test

In general, Terzis grooming test is an important behavioral test used to evaluate the recovery of elbow flexion function in the upper limb after brachial plexus surgery injury in rodents. Briefly, the mouse was sprayed with approximately 2 ml of water on the head and nose to stimulate forelimb movement to remove water, and then placed inside a clear glass cylinder to observe the movement of its upper limbs. Depending on the forepaw position with elbow flexion, recovery of injured upper limb is assessed on a 0–5 scale as follows: 0, non-responsive; 1. The elbow is flexed, not touching the nose; 2. The elbow is flexed, and the front paw can reach the nose; 3. Stretch higher than the nose; 4. Reach out to eyes but not the ears; 5. Reach out to ears and beyond (Fig. 8A). All animals underwent this experiment prior to surgery, and the results were used as a baseline for upper limb motor levels. All injured mice weekly received TGT from the day of surgery until the sacrificial endpoint. If the injury is complete, all injured mice should be scored at 0 within three days post-injury. Otherwise, animals are excluded.

### 2.7.2. Catwalk analysis

The walking capacity of lesion mice were evaluated and analyzed using the Catwalk system (CatWalk XT 9.1, Noldus Information Technology, Wageningen, Netherlands). All tested mice were previously habituated to the runway 1h before the experiment started. Footprint patterns, maximum contact area, and maximum and average footprint intensity were recorded and measured as indicators of walking recovery. Each tested mouse requires at least three runs for data analysis.

## 2.8. Retrograde motoneuron labelling and labeled cells counting

At day 28 and day 56 post-injury, we randomly chose three mice from each group to receive retrograde tracing experiments. Firstly, we exposed the right musculocutaneous nerve follow by isoflurane anesthesia. Visualized by a surgical microscope, 0.5  $\mu$ L of Fluorogold (Hydroxystilbamidine, AAT Bioquest Inc., Sunnyvale, USA; 6 % in ddH<sub>2</sub>O) was slowly and carefully injected into the distal

musculocutaneous nerve (the injection site is located approximately 4 cm away from the crush point). To allow adequate Fluorogold indicator transport to ventral horn motoneurons, all FG-labeled mice were sacrificed 4 days after injection. After the dissection, spinal cord segment C6 of labeled animals were collected and dehydrated in 30 % sucrose for 48 h. 30  $\mu$ m cross-section of the C6 cervical spinal cord were cut using Cryostat (NX50; Thermo Fisher Scientific, Massachusetts, USA). We use a fluorescence microscope equipped with a 405 nm filter to capture high-resolution images (Leica DM6B, Leica, Wetzlar, Germany). The percentage of FG-labeled motoneurons that also GFP<sup>+</sup> in the C6 spinal cord segment were calculated on every fourth section.

## 2.9. Tissue preparation

At day 28 and day 56 post-injury, all mice requiring further immunofluorescence staining were first subjected to deep anesthesia using isoflurane and then intracardiac perfusion was performed sequentially using PBS and 4 % paraformaldehyde fixative solution. After perfusion, we next dissected and harvested the C6 spinal cord segments, 6 mm long musculocutaneous nerves, and biceps brachii for further analysis. All the collected tissue were submerged in a series of gradients of sucrose solutions (10 %, 20 %, 30 %, 24 h for each at 4 °C) for dehydration, follow by at least 3–5 h post fixation. In addition, we need to weigh the biceps brachii to assess the wet weight ratio prior to the post-fixation process. After that, four series of horizontal sections of biceps brachii were cut using a sliding microtome (SM 2010R, Leica, Wetzlar, Germany) at a thickness of 40  $\mu$ m. And then muscle sections were floated in 6-well plates filled with PBS for further immunofluorescence staining. Meanwhile, we embedded the musculocutaneous nerve tissues with OCT compound and kept it in ultra-low temperature freezer. Before immunohistochemistry experiments, the tissue embedding blocks were cut into longitudinal and transverse sections at a thickness of 5  $\mu$ m with a cryostat (NX50; Thermo Fisher Scientific, Massachusetts, USA).

## 2.10. Quantification of axon regeneration and MBP<sup>+</sup> axons

Longitudinal and transverse sections of musculocutaneous nerves can be used directly for the assessment of regenerating axon due to their spontaneous green fluorescence. On the other hand, we only used a musculocutaneous nerve transverse section of 2 mm proximal to the biceps muscle for MBP<sup>+</sup> axon measurements. The slices were firstly washed with PBS three times, 5 min for each, and then continued rinsed with 0.3 % PBS-Triton-100 three times, 15 min for each. Subsequently, nerve sections were incubated with rabbit MBP Antibody (1:500, Thermo Fisher Scientific, Massachusetts, USA) overnight at 4 °C, followed by AlexaFluor 546-conjugated donkey anti-Rabbit secondary antibody (1:1000; Cat# A10040, Thermo Fisher Scientific) for 2 h at room temperature. Immunofluorescence images were captured by Leica DM6B. Every fourth section from each animal are required for axon number calculation.

## 2.11. Quantification of neuromuscular junctions

Every fourth section of biceps brachii were incubated with Alexa Fluor 594-conjugated  $\alpha$ -BT (1:500; Invitrogen) for 30 min. Morphological observation and analysis of motor endplates were performed under a fluorescence microscope. Depending on the degree of integration of pre- and post-synaptic, motor endplates were rated as denervated, partial innervated or full innervated. No overlap between nerve terminal and the  $\alpha$ -BT<sup>+</sup> cluster was regarded as denervated NMJ, whereas full or partial overlap was regarded as innervated NMJ. The ratio of the three kinds of the NMJs, fully innervated, partially innervated and denervated, was compared. Also, total number of reinnervated NMJs in was compare among three-grouping animals.

## 2.12. Electron microscopy

We applied transmission electron microscopy (TEM) to access myelination of axons after injury. Animals were intracardiac perfused with a mixed solution of 2.5 % glutaraldehyde (Sigma–Aldrich, USA) and 2 % PFA in 0.1 M PB, and then right side of musculocutaneous nerve (2 mm proximal to biceps brachialis) were kept at the same fixative for embedding and sectioning. The glutaraldehyde-fixed nerve fibers were

then washed three times in 0.1 M cacodylate buffer and further post-fixed in 1 % osmium tetroxide overnight. Subsequently, tissue samples were dehydrated in a graded ethanol and infiltrated with a half-acetone and half-resin mixture overnight at 4 °C. After overnight penetrating at 4 °C, the nerve was embedded in resin at 60 °C for 72 h. Ultrathin sections of 100 nm thickness were performed by a vibratome and collected in copper mesh, which were then stained with 3 % uranyl acetate and 1 % lead citrate. And the ultrastructure and myelination of the nerve fibers

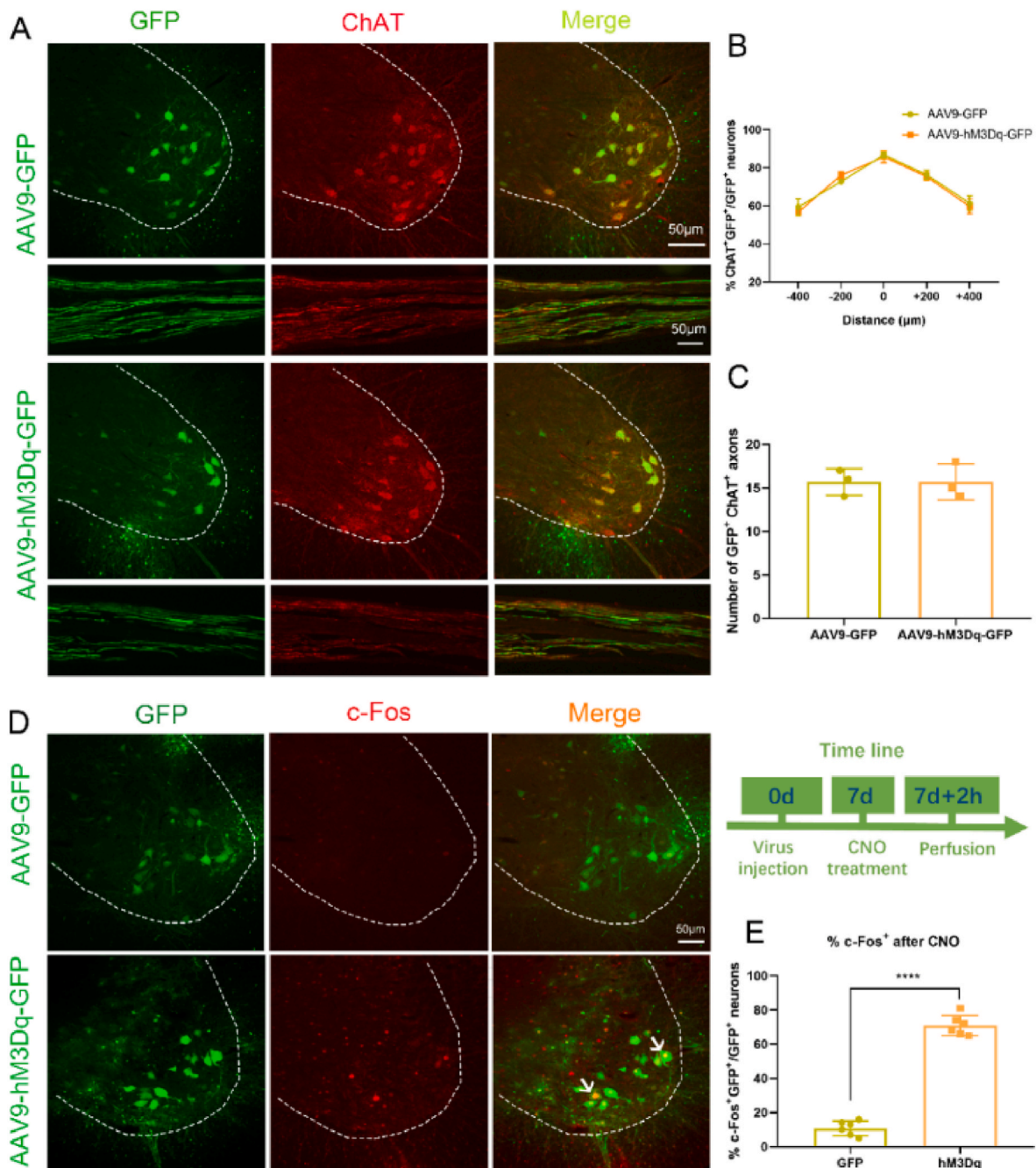


**Fig. 1.** Intraspinal injection of AAV9-hM3Dq primarily transduces motoneurons and hM3Dq<sup>+</sup> motoneurons were activated by CNO treatment. (A) AAV9-hM3Dq-GFP and AAV9-GFP was injected into the right C6 spinal ventral horn. One week later, C6 segment of spinal cord and its ventral root fibers were collected and immunostained for ChAT. Scale bar: 50 μm. (B) Quantification of percentages of GFP<sup>+</sup> motor neurons, “0” indicates the injection point, while “-” indicates rostral side and “+” indicates caudal end. Data are expressed as mean ± SD (n = 3), analyzed by one-way ANOVA analysis of variance followed by Bonferroni’s *post hoc* test. (C) Number of GFP<sup>+</sup>ChAT<sup>+</sup> merge ventral root fibers, data are expressed as mean ± SD (n = 3), analyzed by unpaired t test analysis with two-tailed P-value. (D) The data showed intraperitoneal CNO injection chemogenetically activated hM3Dq<sup>+</sup> neurons *in vivo*. Experiment timeline is shown in the right panel. Very few neurons transduced with AAV-GFP expressed c-Fos while many hM3Dq<sup>+</sup> neurons expressed c-Fos (showed as arrowheads). (E) Quantification of the percentage of GFP<sup>+</sup> neurons that are also c-Fos<sup>+</sup> after CNO administration. Data are expressed as mean ± SD, analyzed by unpaired t test analysis with two-tailed P-value (n = 6; \*\*\*\*p < 0.0001, vs GFP<sup>+</sup>).

were observed and photographed by transmission electron microscope (FEI spirit T12, USA).

### 2.13. Electromyography

Electromyography (EMG) is one of the most important indicators used to estimate the functional restoration of the biceps brachii. Briefly, at day 28 and day 56 post-injury, we exposed the ipsilateral and contralateral sides of musculocutaneous nerve and biceps followed by deep isoflurane anesthesia. After inserting the recording electrode into the biceps muscle and inserting the grounding electrode into the subcutaneous tissue, we gently place the bipolar stimulation electrode on the musculocutaneous nerve. The same density of the stimulus (1 mV, 0.05 ms, 5 Hz) was applied successively to tested animals until at least 20 stable waveforms were obtained. The response of EMG signals was recorded with a multi-channel signal acquisition and processing system (BL-420N, Chengdu, China). A minimum of three independent experiments of each mouse were tested for further analysis.

### 2.14. Statistical analysis

All statistical analyses were performed using GraphPad Prism 8.0 software (GraphPad, San Diego, CA, USA). ImageJ is applied to the quantitative statistics of immunofluorescence images. Data are presented as the mean  $\pm$  standard deviation (SD). Comparisons between the two groups were made using two-tailed Student's t-test. One-way analysis of variance followed by the Tukey's or Bonferroni's post-hoc test was used when more than two groups were compared. Two-way analysis of variance followed by the Tukey post-hoc test was used for comparing multiple groups at different timepoints. The significant difference level was set to 0.05.

## 3. Results

### 3.1. AAV9- hM3Dq virus primarily transduces motoneurons and CNO administration activates mature, hM3Dq<sup>+</sup> motoneurons in vivo

Since the mature motoneurons are the primary neurons that send axons to innervate terminal muscles. We first wanted to determine if the hM3Dq viral could transduce adult motoneurons in the spinal ventral horn. A week after intraspinal injection of AAV9- hM3Dq or AAV9-GFP into the right ventral horn of the C6 segment, we calculated the transduced GFP positive neurons and their extended fiber double-stained with the motoneuron marker, ChAT. The results showed that both AAV9- hM3Dq and AAV9-GFP virus can primarily transduce C6 ipsilateral ventral horn motoneurons (Fig. 1A), with about 85 % of ChAT<sup>+</sup> motoneurons that also labeled by GFP at the injection spot (Fig. 1B and C). Statistically, no significant difference in infection efficiency between AAV9- hM3Dq and AAV9-GFP transduced mice ( $p > 0.05$ ).

To further affirm if the hM3Dq transduced motoneurons could activated by CNO treatment, we administer CNO intraperitoneally to the mice received virus injection a week ago. After a 2-h activation, the mice were sacrificed. And then C6 spinal cord sections were collected and stained with c-Fos. The result showed that CNO administration robustly induce c-Fos expression in hM3Dq<sup>+</sup> neurons. About 71 % of the hM3Dq<sup>+</sup> motoneurons expressed c-Fos, but only 11 % of the GFP<sup>+</sup> motoneurons expressed c-Fos. The difference of the c-Fos positive neurons in C6 ventral horns between the two groups was statistically significant (Fig. 1D and E;  $p < 0.0001$ ). It suggested that the majority of the hM3Dq<sup>+</sup> adult spinal motoneurons can be activated by the CNO.

### 3.2. Chronic chemogenetical activation increased the regeneration of the spinal motoneurons injured by ventral root crush

After confirmation of hM3Dq<sup>+</sup> motoneurons could be activated by CNO administration, we then sought to determine if the activation could

increase the number of regenerative motoneurons. At day 28 and day 56 after C6 ventral root crush injury, we carried out retrograde tracking experiments on injured mice and counted the numbers of FG-labeled neurons in the ventral horn of C6 spinal cord. We found the regeneration of injured motoneurons proceeded with time, showing by the increase of the FG-labeled motoneurons from 38 % at day 28 to 66 % at day 56 in GFP group (Fig. 2C). Importantly, with chronic chemogenetical activation, more motoneuron regeneration occurred in the hM3Dq<sup>+</sup> group, with FG-labeled motoneurons 60 % at day 28 increasing to 75 % at day 56 post-injury. Statistically analysis showed a significantly greater number of FG-labeled motoneurons in the hM3Dq group than that in the GFP group at day 28 post-injury, but not occurred at day 56 post injury. However, even with 8 weeks chemogenetical activation, the FG-labeled motoneurons were still significantly lower than 90 % of the sham group (Fig. 2B and C). The results suggested that chronic chemogenetic activation promote the majority of the C6 ventral horn motoneurons regeneration after root crush.

### 3.3. CNO-induced activated hM3Dq<sup>+</sup> motoneurons accelerates axon extensions after root crush injury

Since axon regeneration is one of the important morphological indicators to measure the recovery of brachial plexus injury, we next investigated whether hM3Dq<sup>+</sup> neuronal activation induced by CNO administration increase the number of regenerating axons. At day 28 and day 56 post injury, the GFP<sup>+</sup> axons within the distal musculocutaneous nerves were counted and measured in 8 mice of each group. As could be found in Fig. 3, more GFP<sup>+</sup> axons were observed in hM3Dq animals than in GFP at day 28 post injury, but there was no significant difference between the two groups at day 56 (Fig. 3B and C). Although the number of regenerating axons increased over time, the number of regenerating axons in injured animals still did not reach the level of healthy mice (Fig. 3C). It can be seen from the results that chronic chemogenetical motoneuronal activation does not guarantee axonal regeneration in injured animals as in healthy animals, it can accelerate axon regrowth in the early stage of injury repair, which may have positive potential for alleviating target organ atrophy.

In addition, we continued to figure out if the growing axons from CNO-activated, hM3Dq<sup>+</sup> neurons successfully make their way to the target organ. To determine this, we collected the biceps brachii from three groups and calculated the regenerating axon fibers at the entrance side of the muscle. Only a few GFP<sup>+</sup> fibers were found in the GFP group at day 28 post injury, while the number of nerve fibers was significantly increased in hM3Dq mice (Fig. 4A and C). However, there are no significance different among three groups at day 56, but the number of regenerating fibers of hM3Dq mice tended to be closer to healthy mice than the GFP mice (Fig. 4C). The above two results are consistent, which means that chronic motoneuronal activation is not only able to accelerate axon regeneration but also make it reach the biceps successfully at first 4 weeks of injury.

### 3.4. Chronic chemogenetic activation improves axonal remyelination and enlarges axon size of the root crush-mice

We next investigated whether the regenerating axon has a healthier structure after recurrent activation of chemogenetic motoneurons. For that, we evaluated the diameter and myelin sheath thickness of regenerating axons under the transmission electron microscopy and measured the number of myelinated axons by Myelin basic protein (MBP) staining. As observed in electron micrographs, hM3Dq mice have the significantly bigger average axon size in the distal musculocutaneous nerve than that in GFP mice at day 28 post injury and also the resemble tendency was shown at day 56 time point (Fig. 5A and B). Notably, there was no significant difference in axon diameter between the hM3Dq group and the sham group at day 56 post surgery, which means that the diameter of regenerating axons after neuronal activation can grow as well as normal

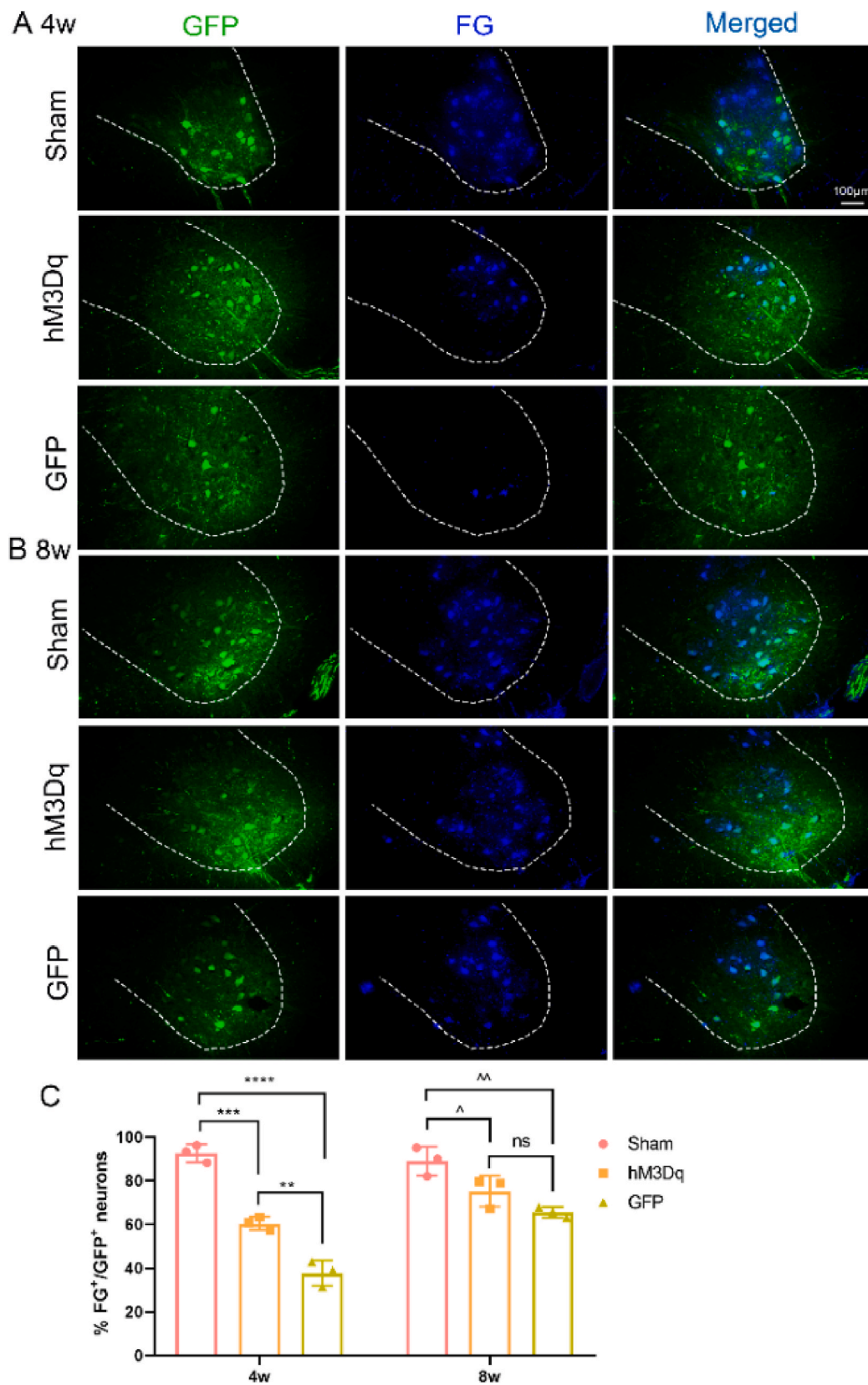


**Fig. 2.** Chronic activation of adult hM3Dq<sup>+</sup> motoneurons increases the number of FG retrograde labeled regenerative motoneurons in vivo (A, B) Representative images of FG-labeled ventral horn motoneurons at day 28 (A) and day 56 (B) post-injury. More FG-labeled motoneurons were observed in AAV9- hM3Dq transfected mice. Scale bar: 100  $\mu$ m. (C) Quantitative analysis of FG-labeled motoneuron number in C6 spinal segment at day 28 and day 56 post-injury. Data are expressed as mean  $\pm$  SD, analyzed by one-way ANOVA analysis of variance followed by the Tukey *post hoc* test. ( $n = 3$ ; \*\*\* $p = 0.0003$  vs. hM3Dq, \*\*\*\* $p < 0.0001$  vs. GFP, \*\* $p = 0.0018$  hM3Dq vs. GFP;  $\wedge p = 0.0111$  vs. hM3Dq,  $\wedge\wedge p = 0.0012$  vs. GFP,  $^{ns} p = 0.1092$  hM3Dq vs. GFP).

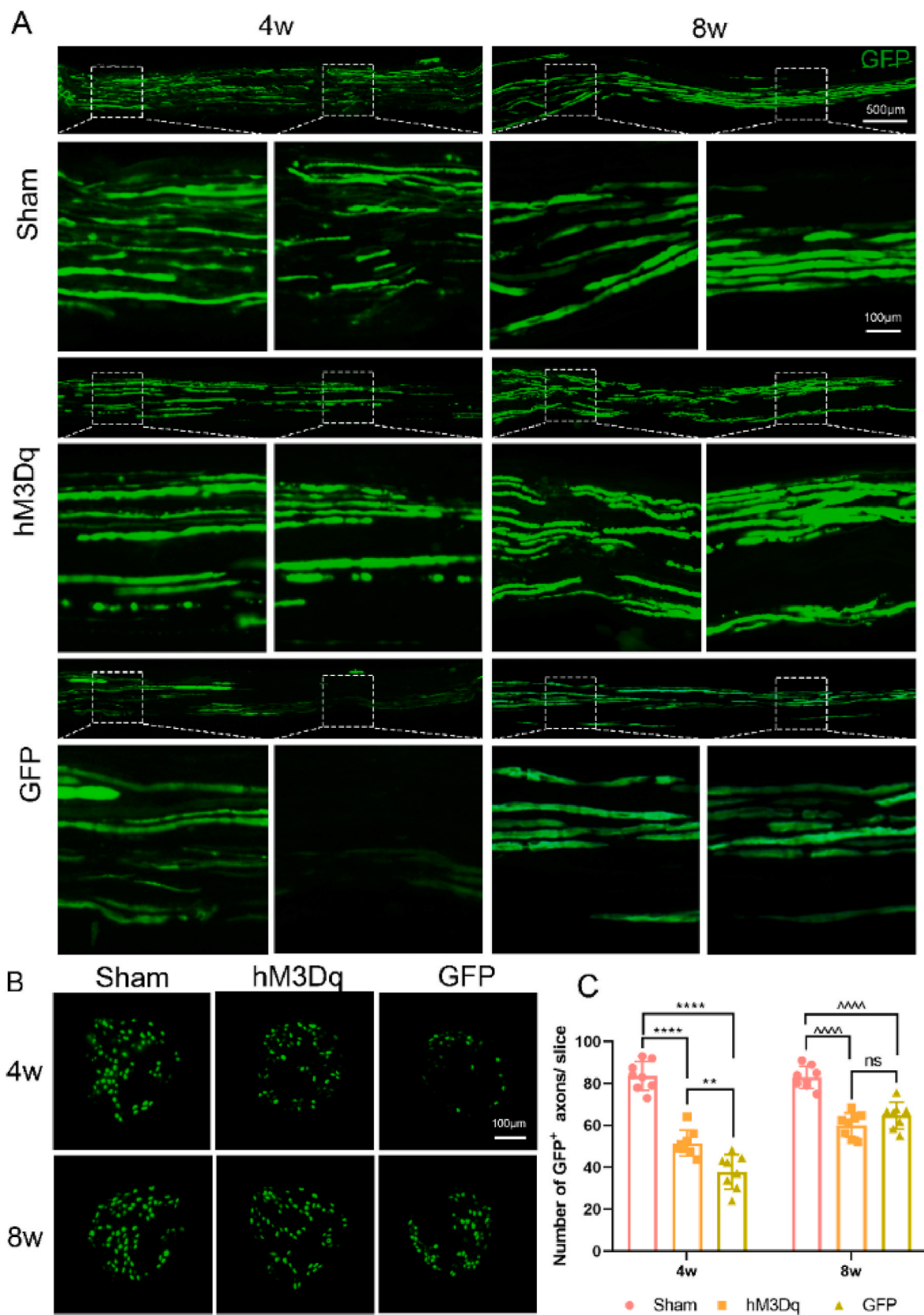


**Fig. 3.** Chronic chemogenetic activation of hM3Dq<sup>+</sup> motoneurons in C6 spinal ventral horns promotes crush-injured axon regeneration (A) Representative images of GFP<sup>+</sup> axons in horizontal sections of the 5 mm musculocutaneous nerve at day 28 and day 56 post-injury. Scale bars: 500 µm in upper row; 100 µm in lower row. (B) Representative images of GFP<sup>+</sup> axons in cross sections of the injured distal musculocutaneous nerve at day 28 and day 56 post-injury. Scale bars: 100 µm. (C) Quantification of GFP<sup>+</sup> axons at day 28 and day 56 post-injury. Data are expressed as mean ± SD, analyzed by one-way ANOVA analysis of variance followed by the Tukey *post hoc* test. (*n* = 8; \*\*\*\**p* < 0.0001 Sham vs. hM3Dq or GFP, \*\**p* = 0.0027 hM3Dq vs. GFP; \*\*\*\**p* < 0.0001 Sham vs. hM3Dq or GFP, *ns* *p* = 0.2880 hM3Dq vs. GFP).

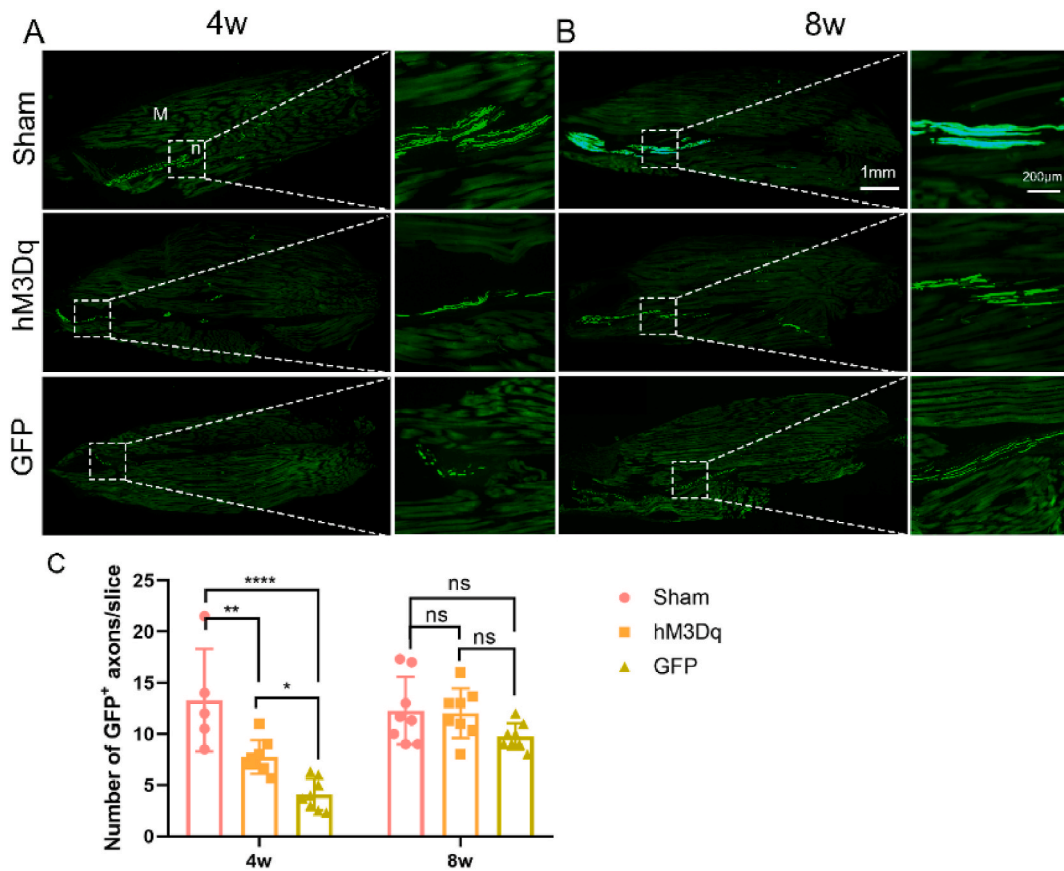


**Fig. 4.** hM3Dq<sup>+</sup> activation accelerates regenerating motor axons extending into the musculocutaneous nerve to innervate the biceps brachialis. (A, B) Representative images of GFP<sup>+</sup> regenerating axons in the musculocutaneous nerve ending in the muscle fibers of the biceps brachialis and their enlarged image at day 28 (A) and day 56 (B) post-injury. Scale bars: 1 mm in the lower magnification on the left column; 200  $\mu$ m in the higher magnification on the right column (M: muscle fibers of biceps; n: musculocutaneous nerve ending). (C) Quantification of numbers of GFP<sup>+</sup> fibers. Data are expressed as mean  $\pm$  SD (n = 5 in sham group at day 28, n = 8 in all other groups; \*\*p = 0.0062 vs. hM3Dq, \*\*\*\*p < 0.0001 vs. GFP, \*p = 0.0406 hM3Dq vs. GFP), analyzed by one-way ANOVA analysis of variance followed by the Tukey *post hoc* test.

mice. Furthermore, axons with different diameters were subdivided and compared among three groups. The result showed more large caliber axons found over time, and diameter distribution of hM3Dq group is more like that of sham mice (Fig. 5C).

The myelin sheath thickness of axons, were also measured and compared. The results indicated that hM3Dq mice have thicker myelin sheath than that of GFP animals at both timepoints (Fig. 5D and E). Besides, the measurement of MBP<sup>+</sup> axon numbers further verify neuronal activation have positive effect to regenerating axons. In hM3Dq mice, an average of  $144.38 \pm 24.28$  MBP<sup>+</sup> axons was present, which is significant higher than  $84.81 \pm 11.80$  of GFP mice at day 28 post injury. Moreover, the same trend was observed at day 56, hM3Dq mice have remarkably more MBP<sup>+</sup> axons than that of GFP mice (Fig. 5F and G). Combined, these data illustrate that chronic chemogenetic activation of injured mature motoneurons could lead to development and maturation of the regenerating axons.

### 3.5. Chronic chemogenetic activation facilitates newly NMJs formation of adult motoneurons injured by ventral root crush

To explore whether chronic chemogenetic activation leads to promoted distal target muscle reinnervation, we next investigate the formation of the new NMJs in the biceps brachialis by immunolabeling with Alpha-bungarotoxin ( $\alpha$ -BT), which specifically binds to acetylcholine receptors [20]. According to the degree of overlap between nerve terminal and Acetylcholine Receptor (AChR) clusters, we divide the observed NMJs into three categories, denervated, partially

innervated, or fully innervated. The NMJ distributions in three groups are shown in Fig. 6C. After counting the double-labeled endplates, we found that numerous fully innervated NMJs in sham animals, more partially innervated and denervated NMJs in the injured animals. With chronic chemogenetic activations, total number of re-innervated motor endplates increases greatly in the later stage of recovery.

At day 28, higher proportion of re-innervated (including partially innervated and fully innervated, totally 52.96 %) motor endplates were observed in hM3Dq group, but only 35.92 % of those in GFP group (Fig. 6A and C). At day 56, there are more denervated NMJs in GFP (28.46 %) than that in hM3Dq (17.26 %) (Fig. 6B and C). As for the calculation of total number of NMJs, no matter at day 28 or 56 post injury, there was no significant difference between hM3Dq mice and sham mice, while the number of NMJs in GFP mice was significantly less (Fig. 6D). Therefore, it suggested that chronic chemogenetic activation of adult motoneurons can significantly promote NMJ reinnervation, thus, facilitating the motor unit repair after ventral root crush injury.

### 3.6. CNO-induced chemogenetic neuronal activation reduces muscle atrophy and promotes electrophysiological recovery of motor unit

To determine the effect of chemogenetic neuronal activation on locomotor function, electrophysiological experiments and target muscle fibers analysis were performed at day 28 and 56 after surgery. After dissection, the left (intact) and right (lesion) biceps brachii of each group of mice were photographed and weighed to access the extent of muscle atrophy following spinal root injury (Fig. 7A and C). Wet weight ratios of



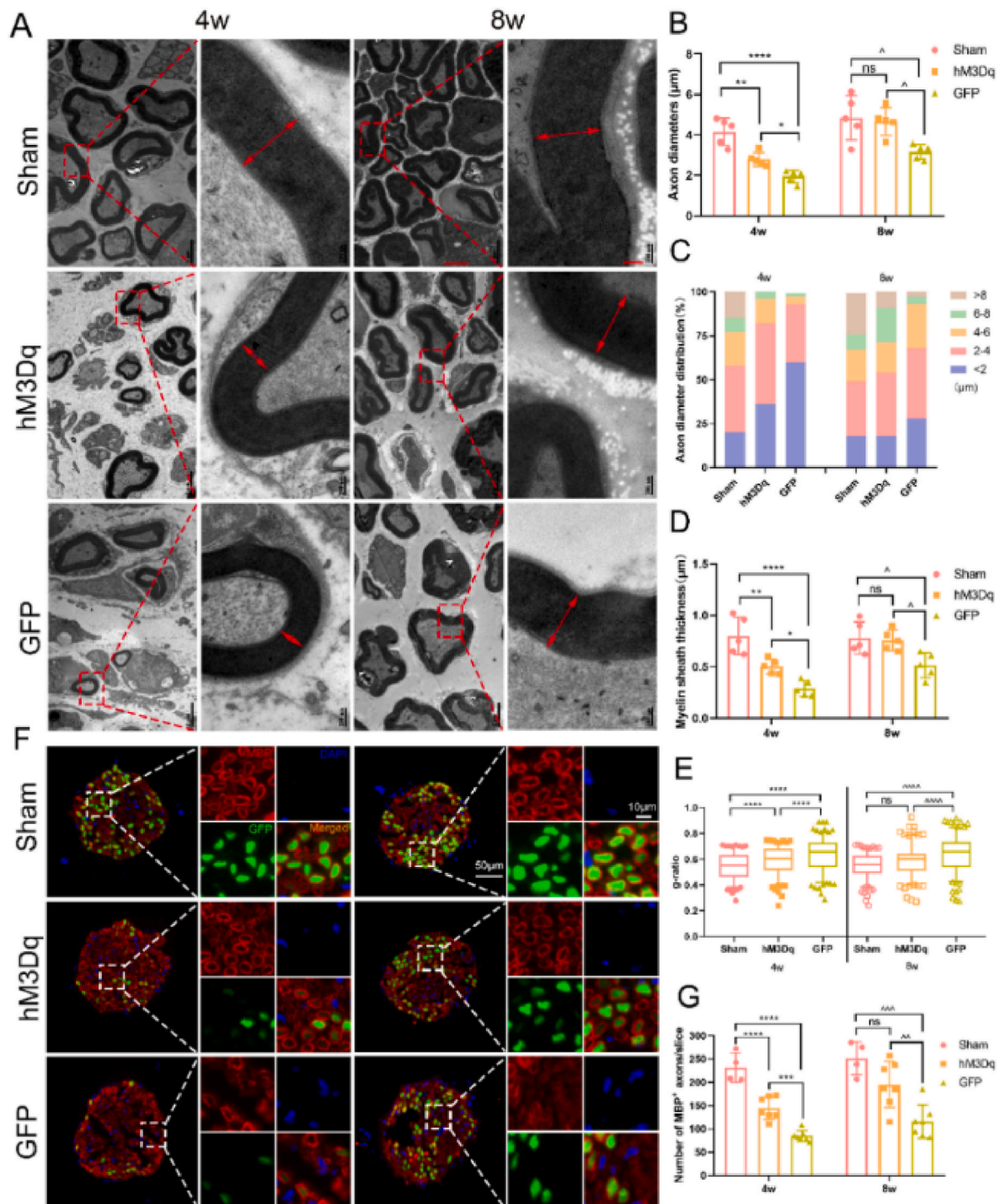


**Fig. 5.** Chemogenetic activation of adult motoneurons improves axonal myelination and enhances cross section area of the regenerative axons after spinal ventral root injury (A) Electron micrographs of distal musculocutaneous nerve. Scale bars: 2 µm in the lower magnification on the left column; 200 nm in the higher magnification on the right column. (B) Quantification of axon diameter of distal musculocutaneous nerve. hM3Dq group show larger axon diameter than GFP ( $n = 5$ ,  $**p = 0.0016$  vs. hM3Dq,  $***p < 0.0001$  vs. GFP,  $*P = 0.0353$  hM3Dq vs. GFP;  $^{ns} p = 0.9319$  vs. hM3Dq,  $^{\wedge} p = 0.0127$  vs. GFP,  $^{\wedge} p = 0.0242$  hM3Dq vs. GFP). (C) Statistical analysis of the proportion of different axonal diameter in injured musculocutaneous nerve at day 28 and day 56 post-injury. (D) Quantification of myelin sheath thickness ( $n = 5$ ,  $**p = 0.0057$  vs. hM3Dq,  $***p < 0.0001$  vs. GFP,  $*P = 0.0408$  hM3Dq vs. GFP;  $^{ns} p = 0.9606$  vs. hM3Dq,  $^{\wedge} p = 0.0178$  vs. GFP,  $^{\wedge} p = 0.0289$  hM3Dq vs. GFP). (E) G-ratio analysis of distal musculocutaneous nerve. (More than 180 axons were measured in all group;  $***p < 0.0001$ ;  $****p < 0.0001$ ,  $^{ns} p = 0.0812$  sham vs. hM3Dq). (F) Cross sections of distal musculocutaneous nerve (stained with MBP, red). Scale bars: 50 µm in the lower magnification on the left; 10 µm in the higher magnification on the right. (G) Number of MBP<sup>+</sup> axons ( $n = 4$  in sham groups,  $n = 7$  in all other groups;  $***p < 0.0001$  vs. hM3Dq, vs. GFP,  $***p = 0.0004$  hM3Dq vs. GFP;  $^{ns} p = 0.1135$  vs. hM3Dq,  $^{***} p = 0.0003$  vs. GFP,  $^{\wedge} p = 0.0075$  hM3Dq vs. GFP). Data are expressed as mean  $\pm$  SD, analyzed by one-way ANOVA analysis of variance followed by the Tukey *post hoc* test.

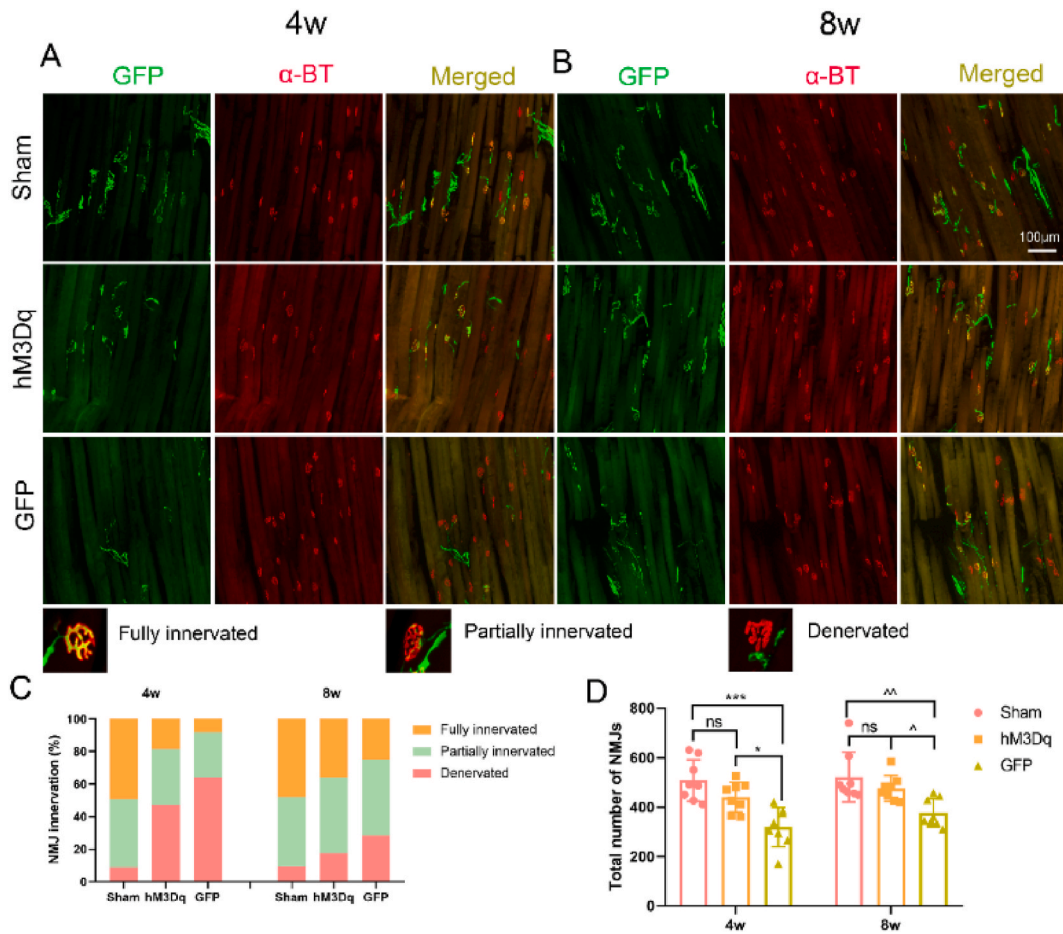


**Fig. 6.** Chronic activation of hM3Dq<sup>+</sup> motoneurons induced by CNO treatment facilitates reinnervation of NMJs at day 28 and day 56 post-injury (A, B) Representative images of NMJs labeled by  $\alpha$ -bungarotoxin (red) and GFP (green) on the biceps brachialis at day 28 (A) and day 56 (B) post-injury. Scale bar: 100  $\mu$ m. (C) Statistical analysis of the proportion of denervated, partially innervated, and fully innervated NMJs at day 28 and day 56 post-injury. (D) Total number of the NMJs on the biceps brachialis. Data are expressed as mean  $\pm$  SD ( $n = 8$ , <sup>ns</sup>  $p = 0.1976$  vs. hM3Dq <sup>\*\*\*</sup>  $p = 0.0002$  vs. GFP, <sup>\*</sup>  $p = 0.0106$  hM3Dq vs. GFP; <sup>ns</sup>  $p = 0.4545$  vs. hM3Dq, <sup>\*\*\*</sup>  $p = 0.0023$  vs. GFP, <sup>^</sup>  $p = 0.0365$  hM3Dq vs. GFP), analyzed by one-way ANOVA analysis of variance followed by the Tukey *post hoc* test.

biceps brachii from the right upper limbs to those from the left were calculated. The ratios were significantly increased in hM3Dq mice, as compared to that in GFP mice at the same time points, suggesting serious muscle atrophy due to inferior nerve recovery in these cases. Importantly, we found that there was no difference in wet-weight ratio between hM3Dq group and sham group at day 56, which implying muscle atrophy of hM3Dq injured mice is mild, similar to that of normal animals (Fig. 7C).

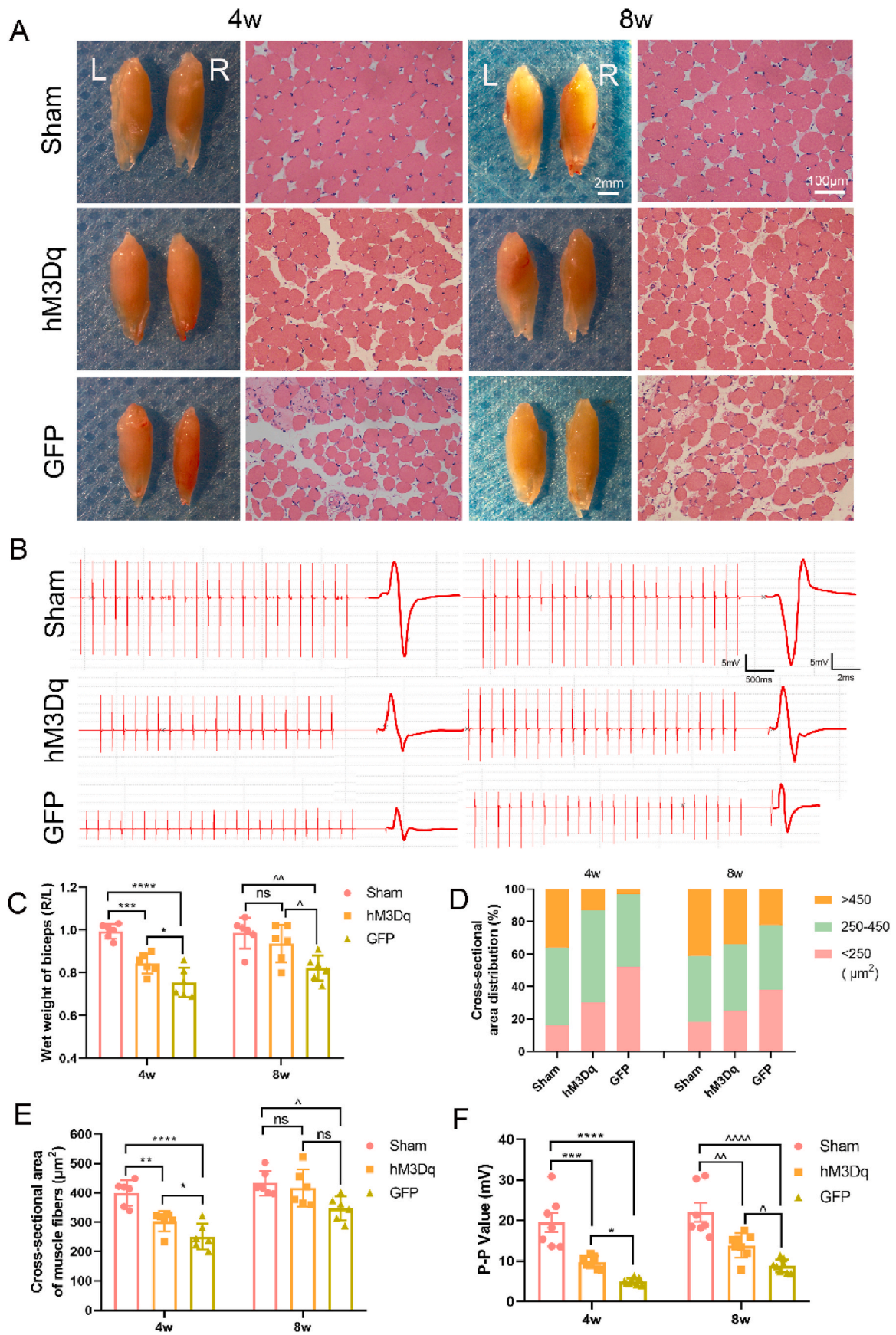
We subsequently evaluate the recovery of biceps brachii by performing HE staining. Cross-sectional areas of myofibers were measured among three groups, the hM3Dq group was almost identical to the Sham group in terms of the distribution of the cross-sectional areas in the later stage of recovery, while it was not happened in the GFP group (Fig. 7D). The quantification of average cross-sectional areas of myofibers also demonstrated the consistent conclusion that neuronal activation does have better effect on muscle recovery. At day 56, no difference between sham and hM3Dq was found with average cross-sectional areas of  $423.79 \mu\text{m}^2 \pm 42.09 \mu\text{m}^2$  or  $416.50 \mu\text{m}^2 \pm 63.45 \mu\text{m}^2$  in each groups, respectively, while the area in the sham group was significantly larger than  $347.14 \mu\text{m}^2 \pm 41.27 \mu\text{m}^2$  in the GFP group (Fig. 7E). Taken together, these data indicate that severe muscle atrophy can be reduced by chemogenetics motor neuron activation.

To further determine the electrophysiological function of reinnervated motor unit, we conducted electrophysiological experiments and recorded compound muscle action potentials (CMAP) in animals at day 28 and day 56 after surgery. The CMAP amplitude of injury mice can't

achieve to the same level of sham mice, but hM3Dq mice show better recovery than GFP mice. Both at day 28 and day 56 after injury, the P-P values of the action potential response in hM3Dq mice were almost twice as high as those in GFP mice, suggesting that chemogenetic neuronal activation led to a remarkably increase in the physiological function of motor units (Fig. 7B and F). Combined, the data further validate the functional recovery of regenerating motor nerves could be improved by our CNO-triggered neuronal activated approach.

### 3.7. Motor functional recovery was improved by chemogenetic neuronal activation

Motor functional rehabilitation is the goal in any therapy for brachial plexus injury. Therefore, we applied Terzis grooming test and catwalk experiment to explore whether chemogenetic neuronal activation can promote the motor function of the upper limbs after cervical spinal root crush injury during the 8 weeks regeneration period. Firstly, the Terzis grooming test [21] was used to evaluate the elbow flexion function of the injured upper limb, and the grading criteria were shown in Fig. 8A. All animals were scored at zero right after they underwent surgery, indicating complete loss of elbow flexion function in the injured animal, whereas they had normal elbow flexion function before surgery. According to the statistical analysis there are signs of recovery within a week in all injured mice, however, the averaged grooming scores of hM3Dq mice began to increase remarkably at 14 days after surgery, and this progression continued until 42 days after surgery, compared with



(caption on next page)

**Fig. 7.** Chronic chemogenetic neuronal activation reduces muscle atrophy and enhances EMG amplitude of re-innervated muscles (A) Representative images of bilateral biceps brachialis (the injured side (R) to the contralateral (L) side) and cross sections of the muscles stained with HE. Scale bars: 2 mm in left column; 100  $\mu$ m in right column. (B) Representative images of EMG response and its individual action potentials. Scale bars: 5 mV in both sides, 500 ms and 2 ms in left and right side respectively. (C) Statistical analysis of the wet weight R/L ratios of biceps ( $n = 6$ ;  $***p = 0.0004$  vs. hM3Dq,  $****p < 0.0001$  vs. GFP,  $*P = 0.0248$  hM3Dq vs. GFP;  $^{ns} p = 0.4839$  vs. hM3Dq,  $\hat{p} = 0.0039$  vs. GFP,  $\hat{p} = 0.0405$  hM3Dq vs. GFP). (D) Distribution of the cross-sectional areas of the muscle filaments in different groups. (E) Quantification of the cross-sectional areas of the muscle filaments ( $n = 6$ ;  $**p = 0.0044$  vs. hM3Dq,  $****p < 0.0001$  vs. GFP,  $*P = 0.0345$  hM3Dq vs. GFP;  $^{ns} p = 0.8407$  vs. hM3Dq,  $\hat{p} = 0.0245$  vs. GFP,  $^{ns} p = 0.0719$  hM3Dq vs. GFP). (F) Averaged P–P value of the lesion side ( $n = 7$  in sham groups,  $n = 8$  in other groups;  $****p = 0.0001$  vs. hM3Dq,  $****p < 0.0001$  vs. GFP,  $*P = 0.0378$  hM3Dq vs. GFP;  $\hat{p} = 0.0018$  vs. hM3Dq,  $****p < 0.0001$  vs. GFP,  $\hat{p} = 0.0449$  hM3Dq vs. GFP). Data are expressed as mean  $\pm$  SD, analyzed by one-way ANOVA analysis of variance followed by the Tukey *post hoc* test.

the GFP group (Fig. 8B). Notably, there are 75 % of hM3Dq with high score ( $\geq 4$ ), implying a good restoration, much higher than 8 % of GFP mice at day 28 after surgery operation.

Meanwhile, we also performed Catwalk experiments throughout the whole rehabilitation process to visualize the walking ability recovery of the mice suffering from spinal ventral root injury, followed by quantification of the footprint data. The footprint and its three-dimensional reflection were shown as Fig. 8C and D, which we can find clear forepaws shape in the sham and hM3Dq mice. On the contrary, although the footprints of the injured upper limbs of the GFP group could be recognized at day 28 post-surgery, they were vague and weak. We then measured the R/L ratios of maximum contact area, maximum intensity and mean intensity as index of walking capacity recovery. Based on the statistical analysis results, although all injured mice have a gradual recovery in walking ability during the regeneration period, hM3Dq mice still performed better than GFP mice, especially in the middle stage of recovery, i.e., at day 21 to day 42 after injury (Fig. 8E–G). These results evidenced that ideal functional recovery of injured mice indeed relate to repeated activation of adult motoneurons, and more importantly, our neuronal activation approach has great potential for the repair of nerve injury.

#### 4. Discussion

Brachial plexus injury is a severe proximal nerve lesion, resulting in a significant functional loss in the affected limb. In previous studies, we and others have developed a variety of treatments that are effective in improving functional recovery after brachial plexus injury, such as administration of small molecule peptide and the delivery of neurotrophic factor [6,8,22]. Most of the studies have focused on systemic pharmacological treatments, and measures that directly and precisely control the regenerating capacity of motoneurons are rarely mentioned. Notably, neuronal activity has been reported to profoundly affect the functional recovery after both central and peripheral nerve system injuries [23,24] by promoting sprouting of spared projections [25,26], enhancing regenerative axonal growth [27,28], improving remyelination [29] and facilitating synaptic formation [30,31]. Numerous tools have been developed to modulate the activity of neurons, including electrical stimulation [32], optogenetic modulation [33], nanomaterial-mediated magnetic [34] and acoustic modulation [35]. While these methods are undoubtedly effective in activating neurons, each method has its own drawbacks. For example, electrical and acoustic approaches have poor capacity to address specific cells and optogenetic methods have short tissue penetration and require an invasive implantation of optical fiber into the organ. Whereupon, the consecutive chemogenetic stimulation is another promising means to modulate neuronal activity in a relatively convenient fashion due to its specific neuronal selectivity and controllable drug activation.

In the present study, we investigated whether chemogenetic neuronal activation can improve regeneration and motor function restoration after cervical spinal ventral root injury. Cervical root injury results in neuronal death within the injured segment, and the surviving neurons must possess robust regenerative capacity to achieve long-distance regeneration and reinnervate target organ [36,37]. We found that chemogenetic motoneuronal activation increase the number regenerating motoneurons and their extending axon at the early stage of

regeneration. Meanwhile, neuronal-activation stimulated recovery of elbow flexion and walking ability of injured mice almost throughout the whole regeneration period. We believed that these motor function improvements were related to an enhance reinnervation of the biceps during the critical recovery stage. Our investigation marks a vital step in demonstrating that modulating neuronal activity can elicit functional benefits following a severe proximal nerve injury.

One of the key reasons for poor regeneration after severe ventral root injury is the gradual degeneration of motoneurons and their attached nerve fiber within a limited time window. In our study, more regenerated neurons were observed at the early stage of recovery, i.e., at the 4-week time point, after neuronal activation according to the result of retrograde labeling experiments, whereas there was no significant difference in the late recovery period, i.e., at the 8-week time point (Fig. 2). Moreover, the regenerating axons from those motoneurons exhibited robust growing ability following motoneuronal-activation, with more fibers extending into the biceps at 4-week after injury, while this effect was not observed at 8-week (Fig. 4). However, our results are contrary to a previous study [19] that showed no axon regeneration at 4-week post dorsal root crush injury while significant regeneration was observed after 12 weeks. We assumed that this difference is due to the fact that their research focuses on the regeneration of the central branches of DRG neurons [38,39], whose functional recovery required the fibers access into the spinal cord, is more difficult to achieve compared to our peripheral branches. Another explanation for this improvement in the early regeneration stage after motor neuron activation is that Schwann cells are supportive for axon regeneration [40,41]. As observed in our results, more myelinated axons were found in hM3Dq mice, and more importantly, these myelinated axons had larger diameters and thicker myelin sheaths (Fig. 5). Our study shows that long-term chronic neuronal activation can accelerate axon regeneration in the early stages of brachial plexus injury, which may effectively prevent muscle atrophy caused by prolonged denervation.

More axons entering a muscle does not mean that more functional synapses are formed [42]. Therefore, the positive effects of chronic motoneuronal activation in our research cannot be limited to enhancing axon regrowth, but also involve rebuilding healthier neuromuscular junctions to maintain long-term motor function. Some studies have shown that neural activity facilitates synaptic formation and plays a key role in the maintenance of precise synaptic connections [18,33]. Interestingly, our chemogenetic activation of hM3Dq<sup>+</sup> motoneurons exhibit similar conclusions. We noticed an improvement of reinnervation in hM3Dq mice at both 4-week and 8-week after injury, supported by evidence of an increased number of neuromuscular junctions (Fig. 6), a reduction in muscle atrophy, and improved electrophysiological function (Fig. 7). It is worth noting that our results showed no significant difference in axon regeneration at the 8-week timepoint, but a significant difference in neurological functional improvement. We believe that this may be due to the fact that the GFP control group exhibited poor axonal regeneration capacity in the early recovery period, and even though the number of regenerating axons in the later period increased, it was difficult to form a functional neuromuscular junction after prolonged denervation of the muscles. In a previous study, evoked EMG responses by neuronal activation were observed as early as 2 weeks after sciatic nerve transection, and its amplitude reached the level of intact animal at 4-week time point, which was sufficient to support a good

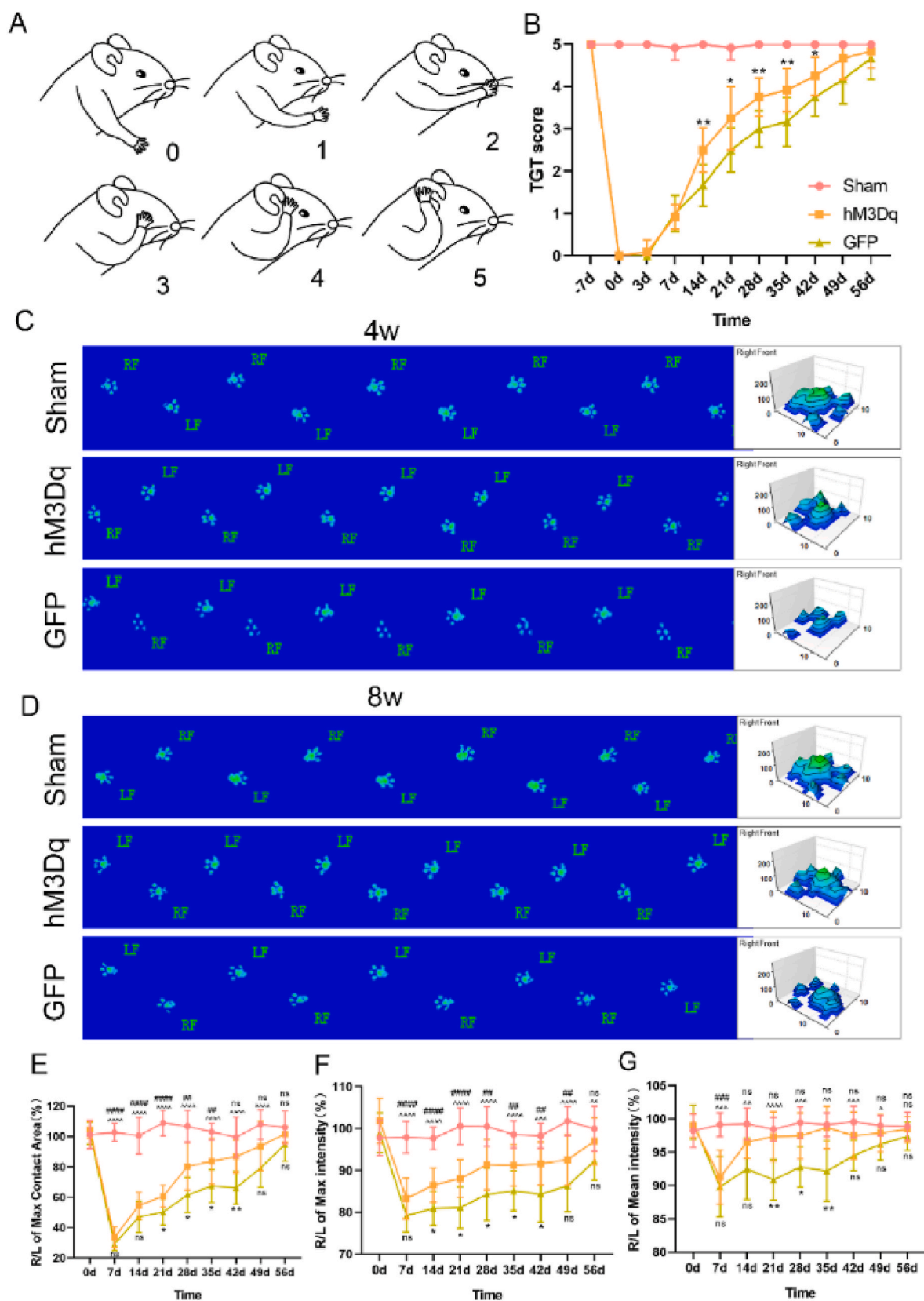


**Fig. 8.** Chronic activation of motoneurons enhances functional recovery of elbow flexion and walking ability post-injury (A) Positions of the forelimbs and corresponding scores (0–5) in the Terzis grooming test (TGT). (B) TGT scores pre- and post-injury ( $n = 12$  in each group;  $*P < 0.05$ ,  $**P < 0.01$  hM3Dq vs. GFP). (C, D) Footprints of the upper limb at day 28 and day 56 post-surgery, RF: right front footprint, LF: left front footprint. (E–G) Percentage of R/L max contact area, R/L max intensity and R/L mean intensity from day 0 to day 56 post injury ( $n = 10$  in each group;  $*P < 0.05$  Sham vs. hM3Dq;  $*P < 0.05$  Sham vs. GFP;  $*P < 0.05$  hM3Dq vs. GFP at the same time point). Data are expressed as the mean  $\pm$  SD, analyzed by two-way ANOVA analysis of variance followed by the Tukey *post hoc* test.

recovery of motor function [43]. Whereupon, our results indicate that although the EMG amplitude was significantly improved in the hM3Dq group at the 4-week time point, it still did not reach the level of normal animals and was closer to normal animals until 8 weeks, while the GFP control group showed a worse electrophysiological response throughout the recovery period (Fig. 7). This slight discrepancy can be attributed to the fact that sciatic nerve injury is a distal nerve lesion and brachial plexus injury is a severe proximal nerve injury, so the former appears to recover more quickly. In any case, the conclusions of the two studies are relatively consistent, showing that a strong EMG response can support the recovery of motor function.

Although our study provides multiple evidence to support that motoneuron activation can increase axon regeneration and improve motor function recovery, it still lacks of mechanistic investigation. According to how chemogenetics technology works, hM3Dq alters neuronal activity by activating the Gq signaling pathway and increasing the intracellular  $Ca^{2+}$  concentration [15]. As  $Ca^{2+}$  play an important role in nerve regeneration, it is generally believed that the neural regeneration caused by neuronal activation is largely related to the enhancement of intracellular calcium concentration [18,33]. We have come to the same conclusion through in vitro DRG explant culture experiments, but this data has not yet been published. Another mechanism is to focus on the functionality of mTOR. mTOR is known to regulate the interaction of dynamic microtubules, which also has positive effect on axonal assembly [44,45]. A previous study has confirmed that DRG neuronal activation can increase mTOR expression to promote axon regeneration [19], but it remains unknown whether motor neurons share the same mechanism. We look forward to further mechanism exploration.

It is widely recognized that the ultimate goal of basic research is to facilitate clinical translational applications. In this context, we will address the clinical application value of our research from two key perspectives: neuronal activation and the use of adeno-associated virus (AAV) vectors. A substantial body of basic research has demonstrated that neuronal activation can facilitate the repair of nervous system injuries, delay the progression of neurodegenerative diseases, and alleviate neuropathic pain [18,46]. However, technical limitations associated with neuronal activation have impeded the advancement of this research area. On the other hand, AAV serves as a gene therapy vector with high efficiency, low immunogenicity, and tissue specificity, and has demonstrated potential for clinical applications in various diseases [47,48]. Our study leverages AAV vectors to achieve specific neuronal activation, thereby mediating the repair of nerve injury and offering a novel perspective for clinical research on these diseases. Therefore, future research will need to enhance the performance of AAV vectors through multidisciplinary collaboration and technological innovation, in order to advance the clinical application of neuronal activation.

## 5. Conclusion

In summary, we have developed a chronic chemogenetic approach to activate hM3Dq<sup>+</sup> motor neurons following brachial plexus injury, thereby accelerating axonal regeneration and promoting functional recovery. This strategy holds promise as a clinical therapeutic approach for treating nervous system injuries.

## Author contributions

WWT, ZLH and LSQ conceived and designed the study. LSQ, WZZ, HY, WPZ, SJQ, WJJ, conducted experiments and analyzed the data. ZLH and LSQ wrote the manuscript. WWT and KZ contributed to the manuscript revision. All authors read and approved the final manuscript.

## Funding

This work was supported by the National Natural Science Foundation of China [No. 82171369]; Guang Dong Basic and Applied Basic Research Foundation [No. 2022A1515110189]; Sun Yat-sen Pilot Scientific Research Fund [No. YXQH202427] and National Natural Science Foundation of China [No. 82404189].

## Declaration of competing interest

The authors declare that they have no known competing financial interests or personal relationships that could have appeared to influence the work reported in this paper.

Lihua Zhou reports financial support was provided by Sun Yat-Sen University. Ke Zhong reports financial support was provided by Sun Yat-Sen Memorial Hospital. Reports a relationship with that includes: Has patent pending to. If there are other authors, they declare that they have no known competing financial interests or personal relationships that could have appeared to influence the work reported in this paper.

## References

- [1] Gutkowska O, Martynkiewicz J, Urban M, Gosk J. Brachial plexus injury after shoulder dislocation: a literature review. *Neurosurg Rev* 2020;43(2):407–23.
- [2] Scheib J, Hoke A. Advances in peripheral nerve regeneration. *Nat Rev Neurosci* 2013;9(12):668–76.
- [3] Rasulić L, Savić A, Živković B, Vitošević F, Mićović M, Bašćarević V, et al. Outcome after brachial plexus injury surgery and impact on quality of life. *Acta Neurochir* 2017;159(7):1257–64.
- [4] He Z, Jin Y. Intrinsic control of axon regeneration. *Neuron* 2016;90(3):437–51.
- [5] Mahar M, Cavalli V. Intrinsic mechanisms of neuronal axon regeneration. *Nat Rev Neurosci* 2018;19(6):323–37.
- [6] Eggers R, de Winter F, Arkenaar C, Tannemaat MR, Verhaagen J. Enhanced regeneration and reinnervation following timed GDNF gene therapy in a cervical ventral root avulsion. *Exp Neurol* 2019;321.
- [7] Ohtake Y, Park D, Abdul-Muneer PM, Li H, Xu B, Sharma K, et al. The effect of systemic PTEN antagonist peptides on axon growth and functional recovery after spinal cord injury. *Biomaterials* 2014;35(16):4610–26.
- [8] Lv SQ, Wu W. ISP and PAP4 peptides promote motor functional recovery after peripheral nerve injury. *Neural Regen Res* 2021;16(8):1598–605.
- [9] Barra B, Conti S, Perich MG, Zhuang K, Schiavone G, Fallegger F, et al. Epidural electrical stimulation of the cervical dorsal roots restores voluntary upper limb control in paralyzed monkeys. *Nat Neurosci* 2022;25(7):924–34.
- [10] Han S, Kim DH, Sung J, Yang H, Park JW, Youn I. Electrical stimulation accelerates neurite regeneration in axotomized dorsal root ganglion neurons by increasing MMP-2 expression. *Biochem Biophys Res Commun* 2019;508(2):348–53.
- [11] Gordon T. Electrical stimulation to enhance axon regeneration after peripheral nerve injuries in animal models and humans. *Neurotherapeutics* 2016;13(2):295–310.
- [12] Chu XL, Song XZ, Li Q, Li YR, He F, Gu XS, et al. Basic mechanisms of peripheral nerve injury and treatment via electrical stimulation. *Neural Regen Res* 2022;17(10):2185–93.
- [13] Willand MP, Rosa E, Michalski B, Zhang JJ, Gordon T, Fahnstock M, et al. Electrical muscle stimulation elevates intramuscular BDNF and GDNF mRNA following peripheral nerve injury and repair in rats. *Neuroscience* 2016;334:93–104.
- [14] Faroni A, Mobasser SA, Kingham PJ, Reid AJ. Peripheral nerve regeneration: experimental strategies and future perspectives. *Adv Drug Deliv Rev* 2015;82-83:160–7.
- [15] Zhang S, Gumpfer RH, Huang XP, Liu Y, Krumm BE, Cao C, et al. Molecular basis for selective activation of DREADD-based chemogenetics. *Nature* 2022;612(7939):354–62.
- [16] Li S, Yang C, Zhang L, Gao X, Wang X, Liu W, et al. Promoting axon regeneration in the adult CNS by modulation of the melanopsin/GPCR signaling. *Proc Natl Acad Sci USA* 2016;113(7):1937–42.
- [17] Lim J-HA, Stafford BK, Nguyen PL, Lien BV, Wang C, Zukor K, et al. Neural activity promotes long-distance, target-specific regeneration of adult retinal axons. *Nat Neurosci* 2016;19(8):1073–84.
- [18] Kawai M, Imaizumi K, Ishikawa M, Shibata S, Shinozaki M, Shibata T, et al. Long-term selective stimulation of transplanted neural stem/progenitor cells for spinal cord injury improves locomotor function. *Cell Rep* 2021;37(8):110019.
- [19] Wu D, Jin Y, Shapiro TM, Hinduja A, Baas PW, Tom VJ. Chronic neuronal activation increases dynamic microtubules to enhance functional axon regeneration after dorsal root crush injury. *Nat Commun* 2020;11(1):6131.
- [20] Mills K. The basics of electromyography. *J Neurol Neurosurg Psychiatr* 2005;76(Suppl 2):ii32–i35.
- [21] Bertelli JA, Mira J-C. Behavioral evaluating methods in the objective clinical assessment of motor function after experimental brachial plexus reconstruction in the rat. *J Neurosci Methods* 1993;46(3):203–8.

- [22] Li H, Wong C, Li W, Ruven C, He L, Wu X, et al. Enhanced regeneration and functional recovery after spinal root avulsion by manipulation of the proteoglycan receptor PTPsigma. *Sci Rep* 2015;5:14923.
- [23] Zhou K, Wei W, Yang D, Zhang H, Yang W, Zhang Y, et al. Dual electrical stimulation at spinal-muscular interface reconstructs spinal sensorimotor circuits after spinal cord injury. *Nat Commun* 2024;15(1).
- [24] Bertels H, Vicente-Ortiz G, El Kanbi K, Takeoka A. Neurotransmitter phenotype switching by spinal excitatory interneurons regulates locomotor recovery after spinal cord injury. *Nat Neurosci* 2022;25(5):617–29.
- [25] Carmel JB, Berrol LJ, Brus-Ramer M, Martin JH. Chronic electrical stimulation of the intact corticospinal system after unilateral injury restores skilled locomotor control and promotes spinal axon outgrowth. *J Neurosci* 2010;30(32):10918–26.
- [26] Carmel JB, Kimura H, Martin JH. Electrical stimulation of motor cortex in the uninjured hemisphere after chronic unilateral injury promotes recovery of skilled locomotion through ipsilateral control. *J Neurosci* 2014;34(2):462–6.
- [27] Goganau I, Sandner B, Weidner N, Fouad K, Blesch A. Depolarization and electrical stimulation enhance in vitro and in vivo sensory axon growth after spinal cord injury. *Exp Neurol* 2018;300:247–58.
- [28] Ward PJ, Clanton SL, English AW. Optogenetically enhanced axon regeneration: motor versus sensory neuron-specific stimulation. *Eur J Neurosci* 2018;47(4):294–304.
- [29] Gautier HOB, Evans KA, Volbracht K, James R, Sitnikov S, Lundgaard I, et al. Neuronal activity regulates remyelination via glutamate signalling to oligodendrocyte progenitors. *Nat Commun* 2015;6(1).
- [30] Jiang YQ, Zaaime B, Martin JH. Competition with primary sensory afferents drives remodeling of corticospinal axons in mature spinal motor circuits. *J Neurosci* 2016;36(1):193–203.
- [31] Krakowiak J, Liu C, Papudesu C, Ward PJ, Wilhelm JC, English AW. Neuronal BDNF signaling is necessary for the effects of treadmill exercise on synaptic stripping of axotomized motoneurons. *Neural Plast* 2015;2015:1–11.
- [32] Liu Y, Li J, Song S, Kang J, Tsao Y, Chen S, et al. Morphing electronics enable neuromodulation in growing tissue. *Nat Biotechnol* 2020;38(9):1031–6.
- [33] Yan J, Wan Y, Ji Z, Li C, Tao C, Tang Y, et al. Motor neuron-specific membrane depolarization of transected peripheral nerves by upconversion nanoparticle-mediated optogenetics. *Adv Funct Mater* 2023;33:2303992.
- [34] Benfenati F, Lanzani G. Clinical translation of nanoparticles for neural stimulation. *Nat Rev Mater* 2021;6(1):1–4.
- [35] Hellman A, Maietta T, Byraju K, Park YL, Liss A, Prabhala T, et al. Effects of external low intensity focused ultrasound on electrophysiological changes in vivo in a rodent model of common peroneal nerve injury. *Neuroscience* 2020;429:264–72.
- [36] Gu HY, Chai H, Zhang JY, Yao ZB, Zhou LH, Wong WM, et al. Survival, regeneration and functional recovery of motoneurons after delayed reimplantation of avulsed spinal root in adult rat. *Exp Neurol* 2005;192(1):89–99.
- [37] Gu HY, Chai H, Zhang JY, Yao ZB, Zhou LH, Wong WM, et al. Survival, regeneration and functional recovery of motoneurons in adult rats by reimplantation of ventral root following spinal root avulsion. *Eur J Neurosci* 2004;19(8):2123–31.
- [38] Wang R, King T, Ossipov MH, Rossomando AJ, Vanderah TW, Harvey P, et al. Persistent restoration of sensory function by immediate or delayed systemic artemin after dorsal root injury. *Nat Neurosci* 2008;11(4):488–96.
- [39] Qiu J, Cafferty WB, McMahon SB, Thompson SW. Conditioning injury-induced spinal axon regeneration requires signal transducer and activator of transcription 3 activation. *J Neurosci* 2005;25(7):1645–53.
- [40] Wan L, Xia R, Ding W. Short-term low-frequency electrical stimulation enhanced remyelination of injured peripheral nerves by inducing the promyelination effect of brain-derived neurotrophic factor on Schwann cell polarization. *J Neurosci Res* 2010;88(12):2578–87.
- [41] Wilhelm JC, Xu M, Cucoranu D, Chmielewski S, Holmes T, Lau KS, et al. Cooperative roles of BDNF expression in neurons and Schwann cells are modulated by exercise to facilitate nerve regeneration. *J Neurosci* 2012;32(14):5002–9.
- [42] Brandon EP, Lin W, D'Amour KA, Pizzo DP, Dominguez B, Sugiura Y, et al. Aberrant patterning of neuromuscular synapses in choline acetyltransferase-deficient mice. *J Neurosci* 2003;23(2):539–49.
- [43] Jaiswal PB, English AW, Chan YS. Chemogenetic enhancement of functional recovery after a sciatic nerve injury. *Eur J Neurosci* 2017;45(10):1252–7.
- [44] Swiech L, Blazejczyk M, Urbanska M, Pietruszka P, Dortmund BR, Malik AR, et al. CLIP-170 and IQGAP1 cooperatively regulate dendrite morphology. *J Neurosci* 2011;31(12):4555–68.
- [45] VanderWeele DJ, Zhou R, Rudin CM. Akt up-regulation increases resistance to microtubule-directed chemotherapeutic agents through mammalian target of rapamycin. *Mol Cancer Therapeut* 2004;3(12):1605–13.
- [46] Yi MH, Liu YU, Liu K, Chen T, Bosco DB, Zheng J, et al. Chemogenetic manipulation of microglia inhibits neuroinflammation and neuropathic pain in mice. *Brain Behav Immun* 2021;92:78–89.
- [47] Wang D, Tai PWL, Gao G. Adeno-associated virus vector as a platform for gene therapy delivery. *Nat Rev Drug Discov* 2019;18(5):358–78.
- [48] Naso MF, Tomkowicz B, Perry WL, Strohl WR. Adeno-associated virus (AAV) as a vector for gene therapy. *BioDrugs* 2017;31(4):317–34.